

## Evidence from atomistic simulations of fluctuation electron microscopy for preferred local orientations in amorphous silicon

S. V. Khare,<sup>a)</sup> S. M. Nakhmanson,<sup>b)</sup> P. M. Voyles,<sup>c)</sup> P. Keblinski,<sup>d)</sup> and J. R. Abelson  
*Department of Materials Science and Engineering, University of Illinois at Urbana-Champaign, Urbana, Illinois 61801*

(Received 5 January 2004; accepted 4 June 2004)

Simulations from a family of atomistic structural models for unhydrogenated amorphous silicon suggest that fluctuation electron microscopy experiments have observed orientational order of paracrystalline grains in amorphous silicon. This order may consist of correlations in the orientation of nearby paracrystalline grains or anisotropy in the grain shape. This observation makes a natural connection to the known growth modes of microcrystalline silicon and may be useful for other materials systems. © 2004 American Institute of Physics. [DOI: 10.1063/1.1776614]

Obtaining information on higher-order atomic correlations from disordered materials has been difficult. Diffraction measurements yield only the two-body correlation function. A recent advance by Treacy and Gibson called fluctuation electron microscopy (FEM),<sup>1</sup> has been shown to be sensitive to two-, three-, and four-body atomic correlations.<sup>1-3</sup> FEM has been used to study medium range order (MRO, defined here as nontrivial three- and four-body correlations) in amorphous Si (*a*-Si) and *a*-Ge samples grown under different experimental conditions.<sup>1,2,4-9</sup> The FEM signal is the statistical variance in the spatial image intensity distribution

$$V(k, Q) \equiv \langle I^2(\mathbf{r}, k, Q) \rangle_r / [\langle I(\mathbf{r}, k, Q) \rangle_r]^2 - 1, \quad (1)$$

where  $I(\mathbf{r}, k, Q)$  is the diffracted intensity at a position  $\mathbf{r}$  in the image measured by hollow-cone dark-field transmission electron microscopy (TEM).  $k$  is a scattering vector magnitude, and  $1/Q$  is proportional to the real-space resolution of the measurements, which was 1.5 nm.<sup>1,2,4-9</sup> An average over different positions  $\mathbf{r}$  is shown as  $\langle \dots \rangle_r$ . In *a*-Si,  $V(k)$  consistently shows two peaks at  $k \approx 3.2 \text{ nm}^{-1}$  and  $k \approx 5.5 \text{ nm}^{-1}$ , the same positions as the first two broad maxima in the structure factor, which appears amorphous for these films.

In conjunction with these experimental results, computational modeling of unhydrogenated Si (or Ge) has shown that *a*-Si (or *a*-Ge) films are not continuous random networks (CRNs),<sup>5,10-14</sup> but appear to consist of nano-sized, strained crystalline grains embedded in a CRN matrix. This model of *a*-Si is called the paracrystalline model (pc-Si).<sup>5</sup> Previous simulations of FEM from pc-Si models show that the magnitude of  $V(k)$  varies with the paracrystallite size and volume fraction, but the first peak is always higher than the second.<sup>5,10</sup> This peak height ratio matches experiments on films of *a*-Si:H deposited by several methods, and pure *a*-Si films sputtered at low substrate temperatures.<sup>3,6</sup> For sputtered *a*-Si films deposited at substrate temperature  $>250^\circ\text{C}$ ,<sup>7</sup> or under ion-bombardment during growth,<sup>9</sup> or for

*a*-Ge films grown by evaporation at room temperature,<sup>4</sup> the second peak is higher. Existing models of pc-Si do not explain these data.<sup>14</sup>

We show that the peak height ratio in FEM is sensitive to orientational order and the shape of the paracrystalline grains. A systematic investigation of several pc-Si model structures shows that the second peak is higher than the first only for models containing a significant volume fraction of grains with a local preferred orientation or with significant shape anisotropy. Thus we show with *a*-Si as a model system that FEM can detect in otherwise amorphous samples, textural and orientational ordering not seen in diffraction experiments. This conclusion is suggested to be general and could be used in the study of other amorphous materials.

Models of pc-Si were constructed with the Wooten, Weiner, and Weaire<sup>15</sup> method as modified by Nakhmanson *et al.*<sup>10,12,13</sup> This method gives realistic models of pc-Si, consistent with experimentally measured structural, electronic, and vibrational properties.<sup>10,12,13</sup> Our models consist of  $N = 1000$  atoms in a cubic box  $5a_{\text{Si}}$  on a side, where  $a_{\text{Si}} = 5.43 \text{ \AA}$  is the *c*-Si lattice constant. A fraction  $f_g$  of the atoms are in  $m$  paracrystalline grains, while  $1-f_g$  atoms are in the CRN matrix. For each value of  $f_g \approx 0.1, 0.2, 0.3, 0.4$ , we constructed three models with  $m = 1, 2, \text{ or } 4$ , giving 12 total models. A CRN model ( $f_g = m = 0$ ) was also constructed. All these models give an average bond-angle of  $109^\circ \pm 10^\circ$ , and a bond length of  $2.35 \pm 0.02 \text{ \AA}$ , characteristic of the best *a*-Si models.<sup>10,13</sup>

To obtain  $V(k, Q)$  for our models, we used a simple kinematic equation<sup>1,3,2,16</sup> for  $I(\mathbf{r}, k, Q)$ ,

$$I(\mathbf{r}, k, Q) = \sum_{i,j} a_Q(\mathbf{r} - \mathbf{r}_i) a_Q^*(\mathbf{r} - \mathbf{r}_j) \int_{-\pi}^{\pi} d\phi \cos(2\pi \mathbf{k} \cdot \mathbf{r}_{ij}), \quad (2)$$

where  $a_Q(\mathbf{p}) \equiv [(g(k)Q^2)/(Q|\mathbf{k}_i||\boldsymbol{\sigma}|)]J_1(2\pi Q|\boldsymbol{\sigma}|)$ .  $\mathbf{k} \equiv \mathbf{k}_f - \mathbf{k}_i$ , and  $\mathbf{k}_i$  and  $\mathbf{k}_f$  are the initial and final wave vectors of the electrons, respectively.  $a_Q$  is the point-spread function of the microscope, which has a characteristic width  $0.61/Q$ , which for all the calculations here is fixed at  $6 \text{ \AA}$ . The Si atoms are located at positions  $\mathbf{r}_i$ ,  $i = 1 \dots N$ , and  $\mathbf{r}_{ij} \equiv \mathbf{r}_i - \mathbf{r}_j$ . The angle between  $\mathbf{k}$  and  $\mathbf{r}_{ij}$  is  $\phi \equiv \arccos [(\mathbf{k} \cdot \mathbf{r}_{ij})/|\mathbf{k}||\mathbf{r}_{ij}|]$ .  $J_1$  is first order Bessel function,  $g(k)$  is the atomic scattering factor of Si, and  $\boldsymbol{\sigma}$  is the component in the image plane of the argu-

<sup>a)</sup>Present address: Department of Physics, University of Toledo, Toledo, OH 43606; electronic mail: skhare@uiuc.edu

<sup>b)</sup>Present address: Department of Physics, North Carolina State University, Raleigh, NC 27695.

<sup>c)</sup>Present address: Department of Materials Science and Engineering, University of Wisconsin, Madison, WI 53706.

<sup>d)</sup>Present address: Department of Materials Science and Engineering, Rensselaer Polytechnic Institute, Troy, NY.

ment  $p$  of  $a_Q$ . To obtain good statistics,  $I(r, k)$  was calculated from each model after rotations spanning the full  $4\pi$  solid angle.  $V(k)$  was then calculated from Eq. (1), averaging over  $r$  and the rotations.

We list here a summary of some basic results.<sup>17</sup> (i) The CRN model  $V(k)$  is a featureless, monotonically decreasing function of  $k$ , as seen earlier.<sup>5,10</sup> (ii) For the 12 pc-Si models  $V(k)$  and  $I(k)$  show two peaks, the first at  $k_1 \approx 3.2 \text{ nm}^{-1}$  and the second one at  $k_2 \approx 5.5 \text{ nm}^{-1}$ . (iii) For a given grain fraction  $f_g$ , the  $V(k)$  signal decreases as the number of grains  $m$  increases from 1 to 4. (iv) For a given  $m$ , the  $V(k)$  magnitude decreases as  $f_g$  decreases. (v)  $V(k)$  is insensitive to small bond angle distortions.

Qualitatively, these results may be explained by looking at Eqs. (1) and (2). If the argument of the cosine in Eq. (2),  $\mathbf{k} \cdot \mathbf{r}_{ij}$ , is an integer for a pair of atoms ( $i, j$ ), there is a large contribution from that pair to  $I(r, k)$ . Equation (1) emphasizes spatial variations (fluctuations) in  $I(r, k)$ , so if  $I(r, k)$  is different at different points in the sample, there are peaks in  $V(k)$  for those values of  $k$ . Due to its tetrahedral coordination, the CRN gives two peaks in  $I(k)$  corresponding to the first and second shell neighbors for each atom.<sup>17</sup> However since the CRN is homogeneous  $V(k)$  shows no peaks. For the pc-Si models,  $I(k)$  shows two peaks just like in the CRN case. Since different regions of the sample have different amounts of crystallinity,  $I(k)$  varies from one region to another. Hence  $V(k)$  shows peaks at those values of  $k$  where this happens, which corresponds to different shells of nearest neighbors.<sup>17</sup> For a fixed  $f_g$ , as  $m$  increases, the pc-Si model becomes more like a CRN and  $V(k)$  decreases. Similarly, for a fixed  $m$ ,  $V(k)$  decreases with decreasing  $f_g$ .

The FEM simulations from model structures do not match the absolute intensities measured in the TEM. This is a universal problem in FEM simulations;<sup>18</sup> due in part to the small size of the model compared to experimental samples. This means that the magnitude of  $V(k)$  is not useful for comparing models to experiment. Nonetheless, the position and relative magnitude of the peaks in  $V(k)$  are accurately simulated.

We now consider the effects of relative grain orientation. Figure 1 shows calculated  $V(k)$  curves for four models of pc-Si and the CRN. The open (closed) circles show a model M1 (M2) with four grains with  $f_g=0.43$ . Model M1 has the grains randomly oriented while M2 has them all aligned along the same crystal axes. M2 has a lower overall magnitude of  $V(k)$  than M1 because it has less spatial variation in diffraction; all of its grains diffract together. As shown in Fig. 1, the second peak for aligned case M2 is higher than its first peak while for M1 the first peak is higher than the second. Similar models, with  $f_g=0.21$  (squares) show no such peak height reversal. A similar result holds for the  $f_g=0.3$  case (not shown). This suggests that a minimum fraction  $f_{gc} \approx 0.4$  of aligned spherical grains is necessary for the second peak to be greater than the first. This does not mean that there is a global preferred orientation in a sample with a large second peak in  $V(k)$ . In calculating  $V(k)$ , each model is rotated many times, so the effective sample consists of locally aligned regions, but is globally isotropic. This observation is consistent with recent measurements of  $V(k)$  which showed no global preferred orientation in the MRO of  $a$ -Si.<sup>8</sup> Shown by crosses in Fig. 1 are experimental data from Ref. 9. The data show somewhat sharper peaks and show peak

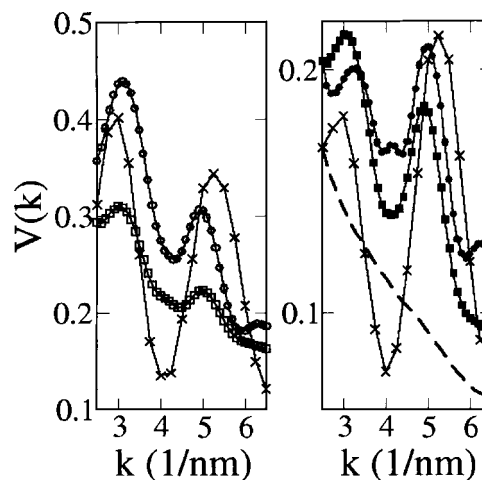


FIG. 1. FEM signal  $V(k)$  for four pc-Si models with  $m=4$  grains occupying a fraction  $f_g=0.43$  (shown by circles) or  $f_g=0.21$  (shown by squares) of the model atoms. The open symbols (left panel) are for models in which the four grains are randomly rotated with respect to one another while the closed symbols (right panel) are for models where all four grains have the same orientation. A CRN is shown by the dashed line. Only models with a large  $f_g$  and aligned grains show the second peak higher than the first. Scaled and shifted experimental data (crosses) for  $a$ -Si films, from Gerbi et al. (Ref.9), measured for ion to neutral flux ratio  $J_+/J_0$  of 13 (25) are shown in the left (right) panel.

height reversal with changing ratio of ion to neutral flux ratio. Our models suggest that this height reversal is caused by increasing orientational order in these films.

Consider now the extreme limits as examples. (i) The solid line in Fig. 2 shows the  $V(k)$  curve for a sphere of perfect Si crystal. Unlike the models in Fig. 1, this model contains no matrix atoms and no strain. The second peak is much higher than the first and split in two near the  $c$ -Si  $\langle 220 \rangle$  and  $\langle 311 \rangle$  reflections. We found similar results for other grain sizes. If the CRN matrix and strain are absent, a single crystal shows a higher second peak. Small strain does not affect this result. (ii) The CRN model (dashed line) in Fig. 1 shows a monotonic decrease in  $V(k)$  with  $k$ . The interplay between these two limits causes either the first peak or second peak to be higher. In the pc-Si models with randomly oriented grains, different grains do not scatter coherently at the same  $k$ , but do so at different directions of  $k$  leading to diffraction

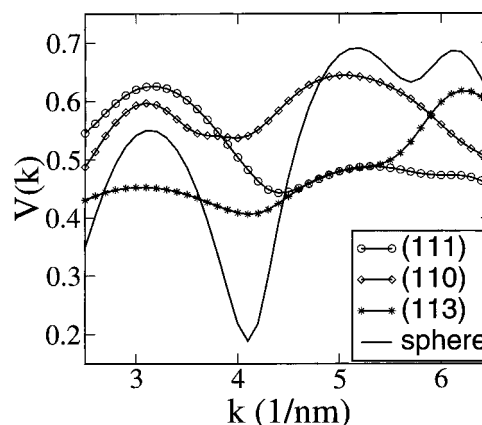


FIG. 2. FEM signal  $V(k)$  for grains of unstrained crystalline Si ( $c$ -Si) with no matrix. The symbols are for cylinders with a length to radius ratio of 0.5 and the cylinder axis along the indicated crystal direction. The solid line is for a sphere. The dependence of relative peak heights on anisotropy of grain shapes is evident.

different from the single crystal limit. When all grains are oriented along the same axis, the second peak is larger than the first, provided there is a sufficient volume fraction of the grains. Our simulation results are consistent with two separate experimental observations: (i) For the same sample, a TEM image containing a Si nanocrystal shows a higher second peak in  $V(k)$  while an area without a crystal shows a higher first peak.<sup>14</sup> (ii) Growing  $\alpha$ -Si with ion-bombardment or increasing substrate temperature brings the growth conditions closer to where micro-crystalline films grow. The second peak of  $V(k)$  has been found to be higher in both these cases.<sup>7,9</sup>

The shape of individual paracrystallites can also influence the relative peak heights. Figure 2 shows  $V(k)$  curves for three cylinders of perfect Si crystal with length  $l$  to radius  $r$  ratio  $l/r=0.5$ . The cylinder axes are along  $\langle 111 \rangle$ ,  $\langle 110 \rangle$ , and  $\langle 113 \rangle$ . The highest peaks  $V(k)$  in each case occur at the  $k$  corresponding to the interplanar spacings parallel to the axis,  $k_{\langle 111 \rangle}=3.2 \text{ nm}^{-1}$ ,  $k_{\langle 110 \rangle}=5.2 \text{ nm}^{-1}$ , and  $k_{\langle 113 \rangle}=6.1 \text{ nm}^{-1}$ . However, a heuristic argument does not suffice to quantify the relative peak height differences.

The higher second peak in  $V(k)$  occurs experimentally under conditions closer to those that produce microcrystalline ( $\mu c$ ) Si. When grown by sputtering,  $\mu c$ -Si tends towards crystallographically textured, elongated, columnar grains.<sup>19</sup> Our current observations suggest that pc-Si films grow in a similar, albeit more disordered manner: they tend toward local orientational order and/or anisotropic grain shapes. This tendency can be suppressed under growth conditions that result in a very disordered film [higher first peak in  $V(k)$ ], but it grows more pronounced as the growth tends toward microcrystallinity. Finally, the ability of FEM to see subtle anisotropy in disordered materials, demonstrated here for  $\alpha$ -Si, may be useful in other materials systems, such as very small semiconductor nanoparticles in a glassy matrix, or electro-optic polymers where a preferred orientation has been introduced by poling.<sup>20</sup>

The authors gratefully acknowledge support from the National Science Foundation under Grant No. DMR02-05858. P.K. acknowledges the support of the National Science Foundation under Grant No. DMR00-74273.

- <sup>1</sup>M. M. J. Treacy and J. M. Gibson, *Acta Crystallogr., Sect. A: Found. Crystallogr.* **A52**, 212 (1996).
- <sup>2</sup>J. M. Gibson, M. M. J. Treacy, and P. M. Voyles, *Ultramicroscopy* **83**, 169 (2000).
- <sup>3</sup>P. M. Voyles, Ph.D. dissertation, Dept. of Physics, University of Illinois at Urbana-Champaign, 2000.
- <sup>4</sup>J. M. Gibson and M. M. J. Treacy, *Phys. Rev. Lett.* **78**, 1074 (1997).
- <sup>5</sup>M. M. J. Treacy, J. M. Gibson, and P. J. Keblinski, *J. Non-Cryst. Solids* **231**, 99 (1998).
- <sup>6</sup>J. M. Gibson, M. M. J. Treacy, P. M. Voyles, H. -C. Jin, and J. R. Abelson, *Appl. Phys. Lett.* **73**, 3093 (1998).
- <sup>7</sup>P. M. Voyles, J. E. Gerbi, M. M. J. Treacy, J. M. Gibson, and J. R. Abelson, *Phys. Rev. Lett.* **86**, 5514 (2001); *J. Non-Cryst. Solids* **293**, 45 (2001).
- <sup>8</sup>P. M. Voyles and D. A. Muller, *Ultramicroscopy* **93**, 147 (2002).
- <sup>9</sup>J. E. Gerbi, P. M. Voyles, M. M. J. Treacy, J. M. Gibson, and J. R. Abelson, *Appl. Phys. Lett.* **82**, 3665 (2003).
- <sup>10</sup>S. M. Nakhmanson, P. M. Voyles, N. Mousseau, G. T. Barkema, and D. A. Drabold, *Phys. Rev. B* **63**, 235207 (2001).
- <sup>11</sup>P. M. Voyles, N. Zotov, S. M. Nakhmanson, D. A. Drabold, J. M. Gibson, M. M. J. Treacy, and P. Keblinski, *J. Appl. Phys.* **90**, 4437 (2001).
- <sup>12</sup>S. M. Nakhmanson, N. Mousseau, G. T. Barkema, P. M. Voyles, and D. A. Drabold, *Int. J. Mod. Phys. B* **15**, 3253 (2001).
- <sup>13</sup>N. Mousseau, G. T. Barkema, and S. M. Nakhmanson, *Philos. Mag. B* **82**, 171 (2002).
- <sup>14</sup>P. M. Voyles and J. R. Abelson, *Sol. Energy Mater. Sol. Cells* **78**, 85 (2003).
- <sup>15</sup>F. Wooten, K. Winer, and D. Weaire, *Phys. Rev. Lett.* **54**, 1392 (1985).
- <sup>16</sup>R. K. Dash, P. M. Voyles, J. M. Gibson, M. M. J. Treacy, and P. Keblinski, *J. Phys.: Condens. Matter* **15**, S2425 (2003).
- <sup>17</sup>S. V. Khare, S. M. Nakhmanson, P. M. Voyles, and J. R. Abelson (unpublished)
- <sup>18</sup>C. B. Boothroyd, *J. Microsc.* **190**, 99 (1998).
- <sup>19</sup>M. F. Cerqueira, M. Andritschky, L. Rebouta, J. A. Ferreira, and M. F. Dasilva, *Vacuum* **46**, 1385 (1995).
- <sup>20</sup>M. L. Ostraat, J. W. De Blauwe, M. L. Green, L. D. Bell, H. A. Atwater, and R. C. Flagan, *J. Electrochem. Soc.* **148**, G265 (2001); D. M. Burland, R. D. Miller, and C. A. Walsh, *Chem. Rev. (Washington, D.C.)* **94**, 31 (1994).